SYNTHESIS OF BiVO4 THIN FILM AS PHOTOANODE WATER SPLITTING AND DYE DEGRADATION

Gunawan[1,✉], R. A. Lusiana[1], A. Haris[1], Y. Astuti[1], E. Pratista, H. Widiyandari[2] and W. Septina[3]

[1]Chemistry Department, Faculty of Sciences and Mathematics, Diponegoro University, 50275, Semarang, Indonesia
[2]Physics Department, Faculty of Mathematics and Natural Sciences, Sebelas Maret University, 57126, Surakarta, Indonesia
[3]National Research and Innovation Agency (BRIN), Jalan M.H. Thamrin Nomor 8, 10340, Jakarta, Indonesia
✉Corresponding Author: gunawan@live.undip.ac.id

ABSTRACT

Synthesis and characterization of $BiVO_4$ thin film as photoanode of PEC water splitting and degradation of methylene blue had been successfully carried out. $BiVO_4$ was obtained from the electrodeposition of BiOI and $VO(acac)_2$. Variations in potential and deposition time were carried out to obtain optimum performance results. $BiVO_4$ results from a potential of -0.2 V for 10 minutes gave the highest photocurrent. Characterization using XRD and SEM showed that the thin film had nanoporous properties. In addition, analysis with UV-Vis DRS obtained a band gap of 2.51 eV. The application of PEC water splitting was carried out with a tandem dual absorber system, $BiVO_4$ as a photoanode, and $CuInS_2$ photocathode providing an operating current of about 0.5 mA/cm². The effect of modification with FeOOH catalyst gave a lower photocurrent compared to using a hole-sacrificing agent. In addition, this system can also produce 99.7% degradation of methylene blue. This showed that $BiVO_4$ had a good potency as PEC water splitting material for hydrogen production and dye waste degradation.

Keywords: $BiVO_4$, PEC Water Splitting, Dye Degradation.

RASĀYAN *J. Chem.*, Vol. 15, No. 4., 2022

INTRODUCTION

Photoelectrochemical (PEC) water-splitting cells have attracted much attention in terms of the conversion of water to hydrogen and oxygen by solar energy.[1] In addition, the PEC system can also decompose industrial dye waste from the resulting •OH production process.

The effectiveness of the PEC system performance is determined by the semiconductor material used in the photoelectrode. $BiVO_4$ is a widely studied semiconductor due to its excellent optical properties, stability, and suitable band edge position.[2,3] $BiVO_4$ thin films can be obtained by various methods such as spray pyrolysis[4,5], ultrasonic spray pyrolysis[6], chemical vapor deposition[7], dip coating[8], hydrothermal[9], and electrodeposition.[10,11] Electrodeposition has easier preparation control and more homogeneous results.[12]

In addition, efforts to improve performance have also been carried out by adding Zn-MOF[13], Fe_2O_3[14], and Fe_2O_3/NiFe-LDH[15] resulting in effective performance. We intended to make a $BiVO_4$ semiconductor photoelectrode with FeOOH modification in this study. $BiVO_4$ was prepared by electrodeposition of BiOI and $VO(acac)_2$.

The success of the synthesis was confirmed by XRD, SEM, and UV-Vis DRS characterizations. The effect of variations in potential, deposition time, and modification with FeOOH as a catalyst was carried out to obtain optimum performance results. The system was then applied to PEC water splitting with a tandem dual absorber system, $BiVO_4$ as photoanode, and $CuInS_2$ photocathode to obtain an optimum current. In addition, the system was also used as a photo fuel cell for methylene blue (MB) degradation.

Thus, it is hoped that this PEC system can play a role in renewable energy and the degradation of dye waste in the environment.

EXPERIMENTAL

Synthesis of BiVO₄ and BiVO₄-FeOOH Thin Films

$BiVO_4$ thin film synthesis was carried out by electrodeposition of BiOI and $VO(acac)_2$ on FTO as shown in Fig.-1. BiOI electrodeposition was made from 50 mL of 0.4 M KI with a pH of 1.3 adjusted with HNO_3 (conc.) then bismuth nitrate was added and the solution was stirred. After the solution was homogeneous, 20 mL of 0.23 M p-benzoquinone in ethanol was added and stirred for 5 minutes. At room temperature Ag/AgCl, Pt, and FTO as reference, counter, and working electrodes were immersed in a previously prepared solution. Before electrodeposition, FTO was cleaned with 1% detergent and sonicated for 14 minutes. After that, rinsed with deionized water and ethanol and then dried with N_2 gas. To remove organic materials, FTO was irradiated with oxygen plasma for 20 minutes. The electrodeposition was run at -0.2 V for 10 minutes. The $BiVO_4$ electrode was made by dropping 0.15-0.2 mL of 0.2 M $VO(acac)_2$ on the BiOI surface electrode, then it was air heated at 450 °C with a ramped temperature of 2 hours and 1 hour after reaching 450 °C. To remove V_2O_5 the electrode was immersed in 1M NaOH for 30 minutes. For modified $BiVO_4$, the synthetic FeOOH-coated $BiVO_4$ was prepared with 0.1 M $FeSO_4$ deaerated with N_2 for 1 hour, and then the $BiVO_4$ was electrodeposited for 10 minutes under illumination at 0.25 V (Ag/AgCl).
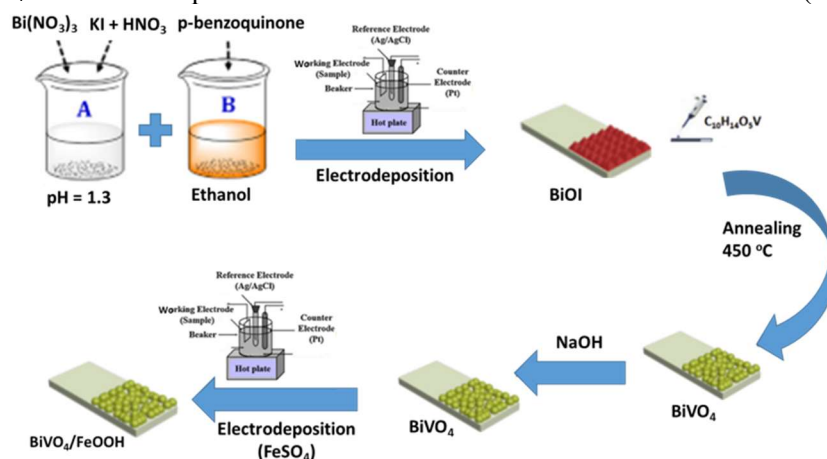

Fig.-1: Schematic Illustration for the Preparation of BiVO₄ and BiVO₄-FeOOH

Characterization of BiVO₄

The successful synthesis of the resulting $BiVO_4$ thin film was confirmed by the peak and crystallinity with X-Ray Diffraction (XRD) Shimadzu XRD-7000. Surface morphology and particle size were observed with a scanning electron microscope (SEM) JSM-6510LA 20 kV Analytical. While the characterization using Shimadzu UV-2430 UV-Vis Diffuse Reflectance Spectroscopy (UV-Vis DRS) was used to analyze the $BiVO_4$ band gap with the Tauc Plot's formula[15] in equation (1):

$$A h\upsilon = (h\upsilon - E_g)^{n/2} \tag{1}$$

The value of n depends on the characteristics of the transition in the semiconductor, i.e. a direct transition (n = 1) or an indirect transition (n = 4). Measurement of the photocurrent response (*J-V*) of $BiVO_4$ was carried out with potentiostat (Hokuto Denko 110) equipped with a digital function generator 0.1 MHz-2MHz DF 1906, Japanese NF (at 0.3 Hz) and Shutter Controller F77 (Suruga Seiki) with a 3-electrode system. Ag/AgCl, Pt, and $BiVO_4$ as a reference, counter, and working electrodes were immersed in Na_2SO_3 solution, respectively. Measurements were made by irradiating light onto the working electrode, with a sweep potential ranging from -0.45 V to +0.4 V and a scan rate of 10 mV/s.

Application on PEC Water Splitting

$BiVO_4$ thin film was measured using a potentiostat (Electrochemical Workstation CorrTest CS Studio 150) under solar simulation (AM 1.5 G, 100 mW cm⁻²) with a three-electrode system ($BiVO_4$ thin film, Ag/AgCl electrode, and Pt electrode as working, reference, and counter electrodes, respectively). The measurements were done from a sweep potential of +1.0 to -0.7 V (vs. Ag/AgCl) with a scan rate of 10 mV/s in phosphate buffer solution at pH 7 with or without sodium sulfite (Na_2SO_3 0.5 M) as a hole scavenger. The resulting $BiVO_4$ was then set in tandem with the $CuInS_2$ photocathode to obtain an unbiased tandem PEC operating

current. The Nernst equation is used to convert the potential obtained into a reversible hydrogen electrode (RHE) through the standard conversion formula as in equation (2)[16]:

$$E_{(RHE)} = E_{(Ag/AgCl)} + E^o_{(Ag/AgCl)} + 0.059 \text{ pH} \tag{2}$$

where $E_{(RHE)}$, $E_{(Ag/AgCl)}$, and $E^o_{(Ag/AgCl)}$ are potential at RHE, potential measured using Ag/AgCl electrode and standard reduction potential of Ag/AgCl electrode (0.1976 V at 25 °C).

Application for Methylene Blue (MB) degradation
The application of $BiVO_4$ as a photoanode cell for the degradation of methylene blue (100 mg/L) was carried out by connecting with a platinum sheet cathode (2 cm × 1 cm) and immersed the two electrodes in MB solution. Then, it was irradiated using a 25 Watt UV lamp (365 nm) at a distance of 20 cm. The effect of variations in treatment time and the type of electrolytes Na_2SO_4 and NaOH were evaluated. The dye concentrations before and after treatment were evaluated using a UV-Vis spectrophotometer at 662 nm.

RESULTS AND DISCUSSION

Synthesis of $BiVO_4$
The preparation of $BiVO_4$ was carried out by electrodeposition using a solution of bismuth nitrate, potassium iodide, and p-benzoquinone to form BiOI and HNO_3. In this case, maintaining acidic conditions using HNO_3 is crucial to dissolve and stabilize Bi ions in the solution.[17] The *J-t* curve profile of BiOI electrode preparation by electrodeposition is depicted in Fig.-2. Then $VO(acac)_2$ was dropped on BiOI to form $BiVO_4$. NaOH solution was used to remove impurities on the surface of the photoelectrode.[12]
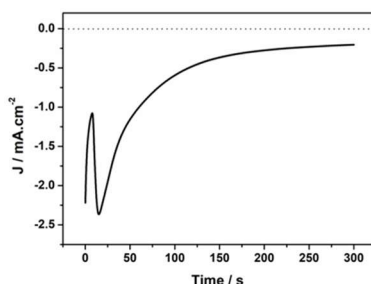

Fig.-2: *J-t* curve of BiOI Electrodeposition on FTO at -0.1V *vs.* Ag/AgCl in 0.23 M *p*-benzoquinone, 0.04 M $Bi(NO_3)_3$, and 0.4 KI Solution

The success of the deposition of BiOI and $BiVO_4$ on FTO can be seen in Fig.-3 with brown BiOI and yellow $BiVO_4$ colors. This was also confirmed by a spectrum with three characteristic linear peaks 2θ at 27.65 °, 38.54 °, and 52.31°. Peaks associated with $BiVO_4$ were obtained at 19.79° (011), 29.65° (121), 31.18° (004), 35.29° (002), 43.85° (015), 48.35° (042), 54.64° (161), and 59.65° (123) which were simulated from monoclinic $BiVO_4$ (JCPDS No.14-0688).[17] The peak patterns of the film samples also match those of Kalanur *et al.* and Park *et al.* [18,19] The peak intensity is not so strong due to the thin $BiVO_4$ deposition. This is also supported by the sharp peaks of the FTO glass (JCPDS No. 46-1088)[20], meaning that the FTO is not covered thickly by $BiVO_4$.
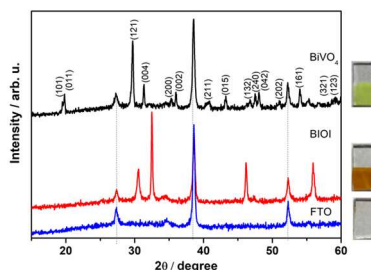

Fig.-3: XRD of FTO, BiOI, and $BiVO_4$.

Figure-4 shows an SEM image of a porous $BiVO_4$ film consisting of aggregated nanoparticles with irregular shapes. The morphology and structure of the $BiVO_4$ sample showed a lax worm-like structure consisting of dense Bi dendrites and Bi dendritic branches.[12,16] This SEM shows that the change in the morphology of

PHOTOANODE WATER SPLITTING AND DYE DEGRADATION   Gunawan *et al.*

the $BiVO_4$ electrode is directly affected by the change in the morphology of the Bi electrode. The different nucleation and growth rates under different depositional states may explain why the morphology of the Bi electrode changes with the applied voltage and temperature.
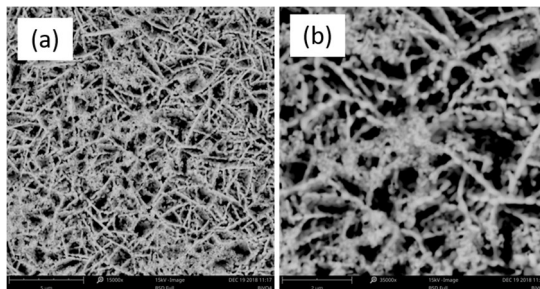

Fig.-4: SEM images of $BiVO_4$ with Magnificent of (a) 15000x and (b) 35000x

Bandgap determination was measured using UV-Vis DRS. Figure-5a shows the spectrum as a function of transmittance and wavelength. The UV-Vis spectrum of the $BiVO_4$ photoanode was shown to have a band edge absorption of about 532 nm similar to the results of Li *et al.*[13] With the Tauc Plots equation,[15] the transmittance was used to determine the $BiVO_4$ band gap as shown in Fig.-5b. From this Figure, the bandgap of $BiVO_4$ is 2.51 eV, which is included in the standard range of several previous studies (2.3-2.6 eV).[12,13]
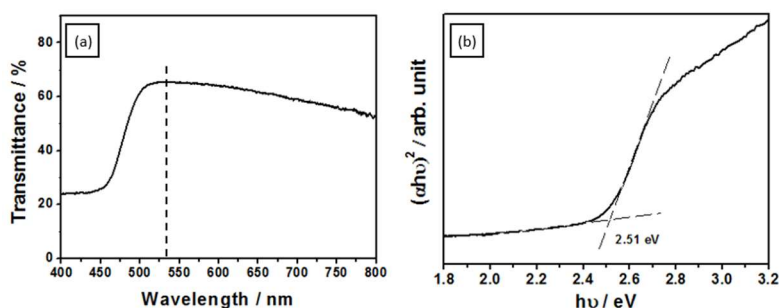

Fig.-5: (a) UV-Vis Spectrum of $BiVO_4$ Measured at 400-800 nm, (b) Bandgap Determination of $BiVO_4$

Photocurrent Response Measurement
Photovoltametry is an efficient method to measure the photoactivity of semiconductors. By scanning the electrode in varied potentials under a chopped light, its current is measured. As a light source, white light lamps or LEDs are usually used with wavelengths in which the semiconductor absorbs a lot. The magnitude of the photocurrent represents the proportion of photogenerated minority carriers that contribute to the photocurrent. As a result, it reveals the presence of surface or bulk traps as well as the external quantum efficiency (EQE). Scan in the dark (light off) to detect pinholes or impurities in the film.[21] The PEC property of $BiVO_4$ in buffer 0.5 M phosphate at pH 7 with 1 M Na_2SO_3 as hole sacrificing agent is shown in Fig.-6, sample 4 as the highest current density. In this work, eight samples were prepared and each sample had a different photocurrent and onset potential. Sample 4 shows the $BiVO_4$ that was prepared resulted in 0.2 V onset potential and photocurrent of 0.85 mA/cm^2 at 1.23V RHE.

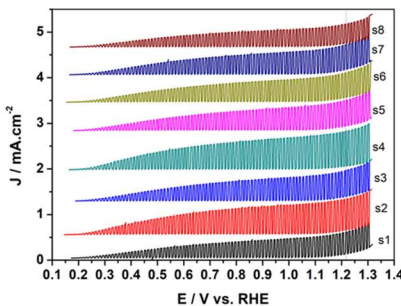Fig.-6: PEC Properties of $BiVO_4$ at pH 7 using Na_2SO_3 Solution as a Hole Sacrificing Agent Illuminated Under 1.5AM chopped Irradiation

PHOTOANODE WATER SPLITTING AND DYE DEGRADATION   Gunawan *et al.*

The effect of heating on the $BiVO_4$ samples was also observed. Samples 1 and 2 were heated in an air atmosphere at 625 ºC for 30 minutes as shown in Fig.-7. Figure-7a shows the effect of post-annealing at 625 ºC for 30 minutes that degrades the current density and onset potential almost twice as of initial samples. Therefore, heating the sample after dropping with VO (acac)$_2$ also needs to be optimized due to different FTO. The stability test of $BiVO_4$ in phosphate buffer solution at pH 7 using 1 M Na_2SO_3 as sacrificing agent is depicted in Fig.-6b. It shows that $BiVO_4$ was stable for 1 hour using hole sacrificing agent, for real oxygen oxidation water splitting it needs a catalyst on its surface. Therefore, if after catalyst introduction the electrode is unstable meaning that the junction between the catalyst and the electrode is not perfect that can degrade the electrode.
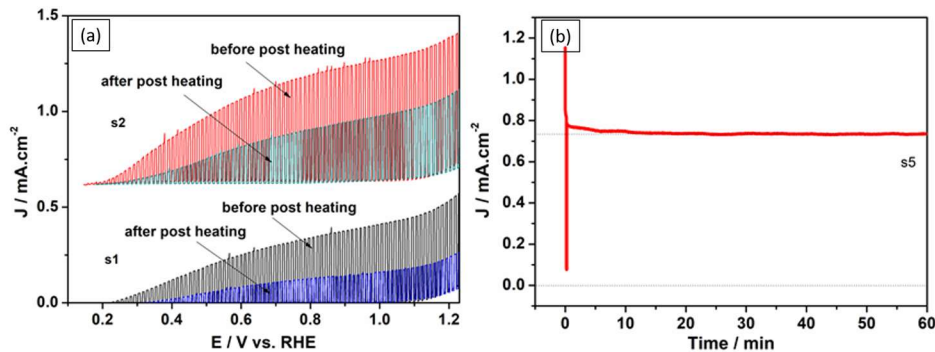

Fig.-7: Effect of Post Heating on Current Density and Onset Potential of $BiVO_4$ Illuminated Under 1.5AM Chopped Irradiation (a), Stability of $BiVO_4$ at 1.21V vs RHE for 60 minutes in 0.5 M Buffer Phosphate and 1M Na_2SO_3 Illuminated Under 1.5AM Irradiation. (b)

The effect of electrodeposition time, voltage, and direction of illumination can be seen in Fig.-8. The Figure shows that front illumination gives a better photocurrent than back illumination for all samples prepared with different voltages and times. It means that the glass coverage of the $BiVO_4$ will reduce the light that goes to the $BiVO_4$ thin film. While the biggest photocurrent 1.97 mA/cm^2 was obtained for the film prepared at -0.2V for 10 minutes.

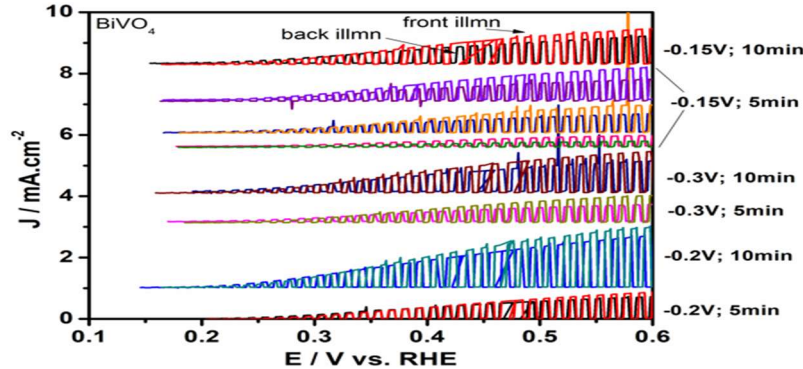Fig.-8: *J-V* Profiles of $BiVO_4$ Prepared with Different Voltage, Time, and the Effect of Position of Illumination to the Photocurrent Responses (backlight and front light) Illuminated Under 1.5AM Chopped Irradiation

The effect of the catalyst on the $BiVO_4$ photoanodes is shown in Fig.-9a with different illumination (from back and front light). Figure-9b shows the real photoanode as photoelectrochemical water splitting, we can see that the photocurrent was reduced compared to using hole sacrificing agent (Na_2SO_3). In this case, bare-$BiVO_4$ and $BiVO_4$-FeOOH were measured using Na_2SO_3 and buffer phosphate pH 6, respectively.

Application of $BiVO_4$ Thin Film Photoanode with Photocathode of $CuInS_2$/In_2S_3-Pt for PEC Water Splitting
The real photoelectrochemical water splitting using photoanode and photocathode can be seen in Fig.-10. We used $CuInS_2$ from our previous work.[22] From the figure, we can see that the operating current for both electrodes was small around 0.5 mA/cm^2 at a potential of 0.5 V. Although the photocathode produces a

PHOTOANODE WATER SPLITTING AND DYE DEGRADATION   Gunawan *et al.*

high current when the onset is too negative it will reduce the operating current. In previous work[23], under the same condition, Pt/In$_2$S$_3$/CdS/CZTS photocathode and BiVO$_4$ photoanode produced a current density around 0.4 mA/cm^2 at a potential of 0.5 V. All of these performance results were still better than those of de Araújo *et al.* and Kubendhiran *et al.* [24,25]
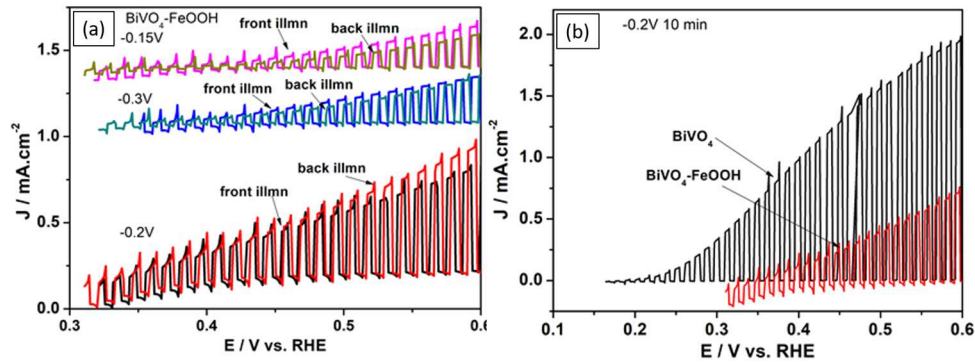

Fig.-9: *J-V* Profiles of BiVO$_4$ with FeOOH Measured at Front and Back Contact Using (a) 0.1 M Buffer Phosphate pH 6, (b) BiVO$_4$ and BiVO$_4$-FeOOH Were Measured Using Na$_2$SO$_3$ and Buffer Phosphate pH 6, Respectively, Illuminated Under 1.5AM Chopped Irradiation
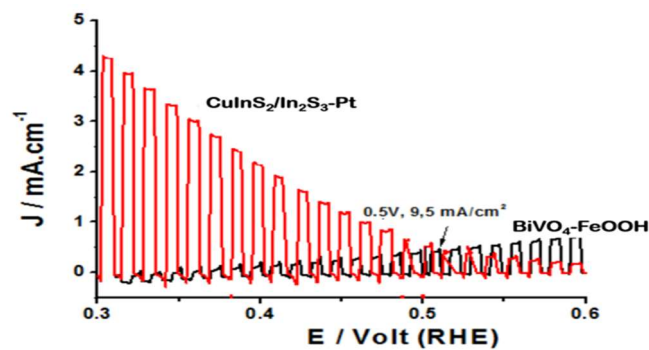

Fig.-10: *J-V* Profiles of BiVO$_4$-FeOOH and CuInS$_2$/In$_2$S$_3$-Pt When Measured Using Solution of Buffer Phosphate pH 6

BiVO$_4$ Thin Film Photoanode in Photo fuel (PFC) Cell for Methylene Blue Degradation
A schematic description of the mechanism for both the PEC degradation of methylene blue and the splitting of water in a BiVO$_4$/FeOOH photoanode system is illustrated in Fig.-11. Due to the presence of the oxidation co-catalyst FeOOH thin film of the composite photoanode, the strong oxidative power of holes (h$^+$) (+2.5V *vs*. RHE) generated in the valence band of BiVO$_4$ upon light irradiation can be efficiently transferred to surface-adsorbed water and hydroxyl groups to generate •OH radicals. In contrast, when an appropriate bias potential was applied to the BiVO$_4$/FeOOH photoanode, photogenerated electrons efficiently move to the external circuit so that •O$_2^-$ can readily form on the cathode. As a result, the simultaneous existence of an external bias and FeOOH oxidation cocatalyst benefits the efficient separation and transfer of the photo-excited electrons and holes and thus effectively improves the degradation efficiency. The photocurrent response demonstrates the thin-film semiconductor's quality. When a semiconductor is illuminated, the higher the photocurrent, the greater the effect to create holes and electrons.[26,27] As a result, dye degradation will be more effective.
Figure-12 depicts the methylene blue (MB) percentage decrease at various light exposure durations. It demonstrates that UV light exposure results in a considerable reduction in MB degradation. At 150 minutes, the percent deterioration of MB is around 90%. Concerning our previous work[23] degradation MB using CdS, under the same conditions at a degradation time of 150 minutes, CdS was able to degrade methylene blue around 21%. From this data, it can be said that BiVO$_4$ is more effectively used to degrade MB compared to CdS.
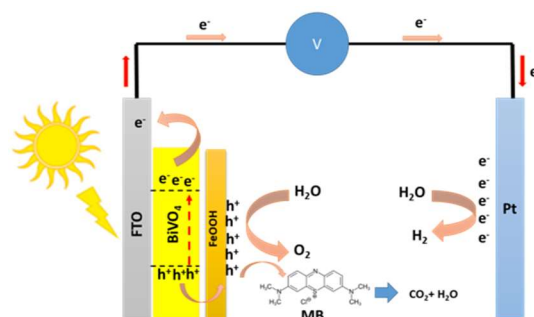
Fig.-11: Schematic of PEC Water Splitting Mechanism and Methylene Blue Degradation with $BiVO_4$/FeOOH Photoanode
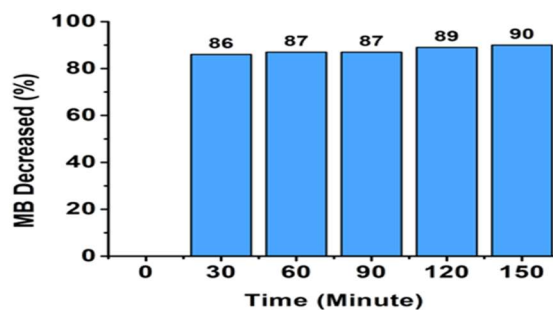

Fig.-12: MB Reduction Using $BiVO_4$ Photoanode at Varied UV-Light Exposure Durations with Na_2SO_4 Solution

The addition of electrolytes increase the methylene blue degradation process as shown in Fig.-13. This is caused by an increase in the solution's conductivity. However, sodium sulfate resulted in the least deterioration, followed by NaOH. Because sodium sulfate has no reaction at the cathode and anode and just serves as an electrolyte that enhances conductivity. Meanwhile, OH$^-$ anions will accelerate the decomposition of MB. When NaOH is employed as the electrolyte, the effect is amplified due to the formation of •OH radicals (from hydroxide ions) and holes in the $BiVO_4$ semiconductor when illuminated.[28] The radical is a potential oxidant that is capable to destruct MB. The results of this study showed similarities with previous studies[23], namely the highest percent degradation of methylene blue occurred in the NaOH electrolyte solution.
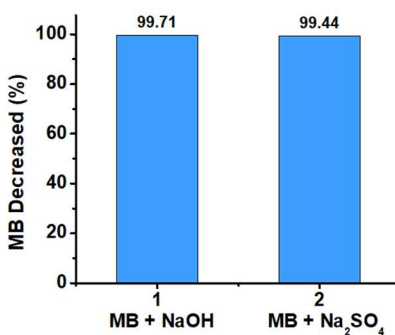

Fig.-13: Graph of MB Degradation Using Different Electrolyte

CONCLUSION

The thin film of $BiVO_4$ can be obtained by electrodeposition of BiOI and followed by nanoparticle deposition using $VO(acac)_2$ to convert BiOI to $BiVO_4$. $BiVO_4$ prepared at potential of -0.2 V for 10 minutes gave the highest photocurrent. The direction of illumination affects the photocurrent produced. Characterization using XRD and SEM shows the thin film prepared was $BiVO_4$ and had a nanoporous property. $BiVO_4$ has a bandgap of 2.51 eV. PEC measurement was done after the deposition of FeOOH as a catalyst on $BiVO_4$ gave a lower photocurrent than using a hole sacrifying agent. PEC measurement using tandem photoanode and photocathode gave an operating current of around 0.5 mA/cm^2. $BiVO_4$ thin film

PHOTOANODE WATER SPLITTING AND DYE DEGRADATION   Gunawan *et al.*

photoanode in a photo fuel cell for methylene blue degradation was obtained the best result around 99.7 % with NaOH electrolyte.

ACKNOWLEDGEMENT

REFERENCES

1. C. M. Kalamaras, A. M. Efstathiou, *Conference Papers in Energy*, Article ID 690627, 1-9(2013), https://doi.org/10.1155/2013/690627
2. J. Jian, Y. Xu, X. Yang, W. Liu, M. Fu, H. Yu, F. Xu, F. Feng, L. Jia, D. Friedrich, R. Van de Krol, and H. Wang, *Nature Communications,* **10**, 2609(2019), https://doi.org/10.1038/s41467-019-10543-z
3. S. Wang, P. Chen, Y. Bai, J.-H. Yun, G. Liu, L. Wang, *Advanced Materials,* **30**, 1800486(2018), https://doi.org/10.1002/adma.201800486
4. F. F. Abdi, N. Firet, R. Van de Krol, *ChemCatChem,* **5,** 490(2013), https://doi.org/10.1002/cctc.201200472
5. Y. Liang, T. Tsubota, L. P. A. Mooij, R. van de Krol, *Journal of Physical Chemistry C,* **115**, 17594(2011), https://doi.org/10.1021/jp203004v
6. M. Li, L. Zhao, L. Guo, *International Journal of Hydrogen Energy*, **35**, 7127(2010), https://doi.org/10.1016/j.ijhydene.2010.02.026
7. E. Alarcon-Llado, L. Chen, M. Hettick, N. Mashouf, Y. Lin, A. Javey, and J. W. Ager, *Physical Chemistry Chemistry Physics,* **16**, 1651(2014), https://doi.org/10.1039/C3CP53904K
8. S. Hernandez, S. M. Thalluri, A. Sacco, S. Bensaid, G. Saracco, N. Russo, *Applied Catalysis A*, **504**, 266(2015), https://doi.org/10.1016/j. apcata.2015.01.019
9. R. Li, F. Zhang, D. Wang, J. Yang, M. Li, J. Zhu, X. Zhou, H. Han, and C. Li, *Nature Communications,* **4**, 1432(2013), https://doi.org/10.1038/ncomms2401
10. P. Hajra, S. Kundu, A. Maity, C. Bhattacharya, *Chemical Engineering Journal*, **374**, 1221(2019), https://doi.org/10.1016/j.cej.2019.06.014
11. M. Zhong, T. Hisatomi, T. Minegishi, H. Nishiyama, M. Katayama, T. Yamada, and K. Domen, *Journal of Materials Chemistry A*, **4**, 9858(2016), https://doi.org/10.1039/C6TA03072F
12. H. Bai, F. Wang, Z. You, D. Sun, J. Cui, and W. Fan, *Colloids and Surfaces A: Physicochemical and Engineering Aspects,* **640**, 128412(2022), https://doi.org/10.1016/j.colsurfa.2022.128412
13. Y. L. Li, Y. Liu, Y. J. Hao, X. J. Wang, R. H. Liu, and F. T. Li, *Materials & Design,* **187**, 108379(2020), https://doi.org/10.1016/j.matdes.2019.108379
14. S. Bai, J. Han, K. Zhang, Y. Zhao, R. Luo, D. Li, and A. Chen, *International Journal of Hydrogen Energy,* **47(7)**, 4375(2022), https://doi.org/10.1016/j.ijhydene.2021.11.122
15. T. B. Li, G. Chen, C. Zhou, Z. Y. Shen, R. C. Jin, and J. X. Sun, *Dalton Transactions*, **40**, 6751(2011), https://doi.org/10.1039/C1DT10471C
16. X. Yang, P. Jiang, Q. Yu, H. Jiang, and X. Xu, *Journal of Alloys and Compounds,* **931**,167428(2022), https://doi.org/10.1016/j.jallcom.2022.167428
17. J. Wang, L. Xu, T. Wang, R. Li, Y. Zhang, J. Zhang, T. Peng, *Advanced Energy Matererial,* **18**, 2003575(2021), https://doi.org/10.1002/aenm.202003575
18. S. S. Kalanur, Y. J. Lee, H. Seo, *Applied Surface Science,* **562**, 150078(2021), https://doi.org/10.1016/j.apsusc.2021.150078
19. Y. Park, K. J. McDonald, K.-S. Choi, *Chemical Society Review,* **42**, 2321(2013), https://doi.org/10.1039/C2CS35260E
20. Z. Wang, X. Li, H. Ling, C. K. Tan, L. P. Yeo, A. C. Grimsdale, A. I. Y. Tok, *Small*, **14(20)**, 1800395(2018), https://doi.org/10.1002/smll.201800395
21. S. Hejazi, M. Altomare, P. Schmuki, *Zeitschrift Für Physikalische Chemie,* **234(4)**, 615(2020), https://doi.org/10.1515/zpch-2019-1479
22. Gunawan, A. Haris, H. Widiyandari, D. S. Widodo, W. Septina and S. Ikeda, *Rasayan Journa of Chemistry,* **14(2)**, 1322(2021), http://dx.doi.org/10.31788/RJC.2021.1425818
23. Gunawan, A. Haris, D. S. Widodo, L. Suyati, W. Septina, *Indonesian Journal of Chemistry,* **21(1)**, 97(2020), https://doi.org/10.22146/ijc.53131

24. M. A. de Araújo, D. Coelho, L. H. Mascaro, and E. C. Pereira, *Journal of Solid State Electrochemistry*, **22(5)**, 1539(2018), https://doi.org/10.1007/s10008-017-3774-1
25. S. Kubendhiran, R. J. Chung, S. Yougbaré, L. Y. Lin, *International Journal of Hydrogen Energy*, **47(63)**, 27012(2022), https://doi.org/10.1016/j.ijhydene.2022.06.048
26. N. P. Diantariani, I. Kartini, A. Kuncaka, and E. T. Wahyuni, *Rasayan Journal of Chemistry,* **13(1)**, 747(2020), http://dx.doi.org/10.31788/RJC.2020.1315597
27. D. I. Prajapati, H. S. Sharma, R. Ameta, *Rasayan Journal of Chemistry,* **11(3)**, 1311(2018), http://dx.doi.org/10.31788/RJC.2018.1132071
28. F. Jiang, Gunawan, T. Harada, Y. Kuang, T. Minegishi, K. Domen, and S. Ikeda, *Journal of American Chemical Society,* **137(42)**, 13691(2015), https://doi.org/10.1021/jacs.5b09015

[RJC-7058/2022]